Applied Catalysis A: General 445–446 (2012) 195–203

Contents lists available at SciVerse ScienceDirect

Applied Catalysis A: General

journal homepage: www.elsevier.com/locate/apcata

# Optimal Ir/Pt ratio for the ring opening of decalin in zeolite supported catalysts

Silvana A. D'Ippolito, Laura B. Gutierrez, Carlos L. Pieck*

*Instituto de Investigaciones en Catálisis y Petroquímica (INCAPE) (FIQ-UNL, CONICET), Santiago del Estero 2654, S3000AOJ Santa Fe, Argentina*

ARTICLE INFO

*Article history:*
Received 2 January 2012
Received in revised form 14 August 2012
Accepted 17 August 2012
Available online 1 September 2012

*Keywords:*
SRO decalin
Ir–Pt/HY zeolite
Diesel

ABSTRACT

The aim of this study was to study the ring opening of decalin at 300 and 350 °C using Pt–Ir/HY zeolite catalysts. Monometallic Ir($x$ = 1.0, 1.5 wt%) and Pt($y$ = 1.0, 1.5 wt%) and bimetallic Ir(1.0)Pt($y$ = 0.5, 1.0, 1.5 wt%), Ir(1.5)Pt($y$ = 0.5, 1.0, 1.5 wt%) catalysts were prepared and catalytically tested. Catalysts were characterized by TPR, pyridine TPD, CO–FTIR, XRD, cyclohexane dehydrogenation and cyclopentane hydrogenolysis activity tests. It was found that the acidic character of Ir oxides species increased the amount of strong acid sites of the support. On the other hand, the Pt content increase favored the formation of medium strength acid sites. The catalysts with higher content of Ir had the higher hydrogenolytic activity while an increase in the Pt content decreased the hydrogenolytic activity. The presence of Pt promoted the dehydrogenation of cyclohexane. Higher yields of dehydrogenated products and increased conversion of cis-decalin were observed at the highest temperature level. The zeolite structure was partially collapsed in the case of the Ir(1.5)Pt(1.5) catalyst. Ir(1.0)Pt(1.0) catalysts at 350 °C and Ir(1.5)Pt(1.5) catalysts at 300 °C, which showed a good performance, seem to have an adequate balance between metal and acid functions that favors the opening of naphthenic rings.



## 1. Introduction

Cetane index (CI) is the key parameter for diesel fuels to secure a proper combustion quality which leads to a lower level of $NO_x$ and particulate matter emissions [1]. The selective ring opening (SRO) is a viable technology to improve diesel quality through an increase in CI. The SRO of bicyclic naphthenes such as decalin is very important in the processing of LCO (light cycle oils) cuts obtained from FCC to improve CI. This improvement cannot be achieved only by the hydrogenation of aromatics since the naphthenes produced have relatively low CI values. Both metallic and acid monofunctional catalysts have been used for SRO but bifunctional ones seem to be more suitable for this process [2]. Onyestyák et al. [3] and McVicker et al. [4] studied the ring opening (RO) of alkyl substituted $C_6$–$C_{10}$ mononaphthenes extensively and found that Ir addition to the catalyst is highly beneficial.

For monofunctional acidic catalysts, it is accepted that the ring opening of $C_6$ and $C_7$ naphthenes occurs on Brønsted sites and starts with a protolytic cracking followed by chain reactions of formed carbenium ions [5–7]. The well-known mechanism accepted for the cracking and isomerization of alkanes on acid catalysts [8–12] can also apply to similar reactions of naphthenes with saturated C—C bonds. Both experimental data and theoretical calculations support the existence of a complex reaction pattern with many catalytic steps: protolytic cracking or dehydrogenation, hydride transfer, skeletal isomerization, β-scission and alkylation of adsorbed ions for this catalyst type [13,14]. The ring opening of more complex (bicyclyc) naphthenes has not been so widely studied.

Zeolites with big sized pores (USY, beta, mordenites) as ring opening catalysts are more selective to RO products as compared to middle pore size ones; consequently, this parameter is very important in RO catalysis [15]. Corma et al. [16] found that zeolite topology has a strong influence on diffusion and therefore on product distribution. Zeolites of higher pore size such as HY are more suitable for the SRO of decalin.

Catalyst acidity is required for the ring opening of multicyclic naphthenes such as decalin. On the contrary, monocyclic naphthenes such as cyclohexane can be broken on monofunctional metallic catalysts [17]. Kubicka et al. [18,19] found an important influence of acidity in the SRO of bicyclic naphthenes. The presence of Brønsted sites is required for ring opening and isomerization [18,19]. The formation of RO products increases as the Pt loading (i.e. metal/acid ratio) increases [20].

The main goal of this work is to determine the influence of total metal loading and Ir/Pt ratio on the ring opening of decalin using bifunctional Pt–Ir/HY catalysts.

## 2. Experimental

### 2.1. Ir(x)–Pt(y) catalysts

A non-commercial NaY zeolite (Si/Al = 3.16, provided by R&D Center, Petrobrás, CENPES) was used as support. The starting material was exchanged with aqueous $NH_4Cl$ 2.2 M with constant

* Corresponding author. Tel.: +54 342 4533858; fax: +54 342 4531068.
*E-mail address:* pieck@fiq.unl.edu.ar (C.L. Pieck).

0926-860X/$ – see front matter © 2012 Elsevier B.V. All rights reserved.
http://dx.doi.org/10.1016/j.apcata.2012.08.037

stirring during 2 h. The solid was filtered and washed with pure water. This procedure was repeated and the resulting solid was dried in an oven at 120 °C overnight. The dried solid was then calcined under air (2 h at 500 °C, heating rate 2 °C $min^{-1}$), the final Si/Al ratio of the material obtained being 3.7, measured by the ICP technique. Metallic precursor salts ($H_2PtCl_6$ and $H_2IrCl_6$ aqueous solutions) were added by simple impregnation (monometallic catalysts) or coimpregnation (bimetallic catalysts) in order to obtain the desired metal percentages (Ir: $x$ = 1.0 wt%, 1.5 wt%; Pt: $y$ = 0.5 wt%, 1.0 wt%, 1.5 wt%) and their combinations. After impregnation, the samples were oven dried at 120 °C, calcined (3 h at 300 °C under flowing dry air) and reduced (2 h at 300 °C under flowing $H_2$). Two series of catalysts were prepared: Ir(1.0)Pt($y$ = 0.5, 1.0, 1.5 wt%) and Ir(1.5)Pt($y$ = 0.5, 1.0, 1.5 wt%) in this way. As all the catalysts were supported on zeolite HY, hereafter the catalysts will be denominated Ir($x$)Pt($y$).

### 2.2. Determination of Si/Al ratio and sodium content

The Si/Al ratios of zeolites were determined by ICP (Perkin Elmer, Optima 2100 DV) while the sodium percentage of the zeolites and supported metal catalysts was determined by atomic absorption spectroscopy using a Perkin Elmer 3110 equipment after acid digestion.

### 2.3. Temperature-programmed reduction (TPR)

These tests were performed in an Ohkura TP2002 equipment with a thermal conductivity detector. At the beginning of each TPR test the catalyst samples were pretreated in situ by heating in air at 400 °C for 1 h. Then they were heated from room temperature to 700 °C at 10 °C $min^{-1}$ in a gas stream of 5.0% hydrogen in argon.

### 2.4. Fourier transform infrared (FTIR) absorption spectroscopy of chemisorbed CO

The Fourier transform infrared spectra of adsorbed CO were obtained to study the effect of Ir deposition on the metallic phase. FTIR spectra of chemisorbed CO for the prepared catalysts were recorded within the wavenumber range of 4000–1000 $cm^{-1}$. A Shimadzu Prestige-21 spectrometer with a spectral resolution of 4 $cm^{-1}$ was used, and spectra were recorded at room temperature. Self-supported wafers with a diameter of 16 mm and a weight of 20–25 mg were used. The experimental procedure was as follows: Catalyst samples were reduced under hydrogen flow at 400 °C (reached at a 10 °C $min^{-1}$ heating rate) for 30 min. Samples were then degassed at $2.7 \times 10^{-3}$ Pa and 400 °C for 120 min. After an initial (I) spectrum had been recorded, the samples were exposed to a $4 \times 10^3$ Pa CO atmosphere for 5 min, and then a second (II) FTIR spectrum was recorded. The chemisorbed CO absorbance for each sample was obtained by subtracting spectrum I from spectrum II.

### 2.5. X-ray diffraction

The analysis was performed with a Shimadzu XD-D1 diffractometer. Diffraction patterns were recorded using Cu Kα radiation filtered with Ni in the 10–60° range at a scan rate of 2° $min^{-1}$, operating at 30 kV and 40 mA.

### 2.6. Temperature-programmed desorption of pyridine

Samples of 200 mg were impregnated with an excess of pyridine. Once the excess had been removed, physisorbed pyridine was eliminated by heating the sample in a nitrogen stream at 110 °C for 1 h. Then, the temperature was raised at a rate of 10 °C $min^{-1}$ to a final value of 650 °C. To measure the amount of desorbed pyridine, the reactor exhaust was connected to a flame ionization detector.

### 2.7. Cyclopentane hydrogenolysis

Before the reaction the catalysts were reduced for 1 h at 500 °C in $H_2$ (60 $cm^3$ $min^{-1}$). Then they were cooled in $H_2$ to the reaction temperature (300 and 350 °C). The other conditions were: catalyst mass = 100 and 150 mg, pressure = 0.1 MPa, $H_2$ flow rate = 40 $cm^3$ $min^{-1}$, cyclopentane flow rate = 0.483 $cm^3$ $h^{-1}$. The products were analyzed chromatographically in a Varian 3400 CX chromatograph equipped with a capillary column (Phenomenex ZB-1) and a conventional FID.

### 2.8. Cyclohexane dehydrogenation

The reaction was performed in a glass reactor with the following conditions: catalyst mass = 50 mg, temperature = 300 °C, pressure = 0.1 MPa, $H_2$ = 36 $cm^3$ $min^{-1}$, cyclohexane = 1.61 $cm^3$ $h^{-1}$. Before the reaction was started the catalysts were treated in $H_2$ (36 $cm^3$ $min^{-1}$, 500 °C, 1 h). The products were analyzed by capillary GC as described before.

### 2.9. Selective ring opening (SRO) of decalin

All SRO experiments were performed in a stainless steel, autoclave-type stirred reactor. The reaction conditions were: temperature: 300 and 350 °C, hydrogen pressure: 3 MPa, stirring rate: 1360 rpm, volume of decalin: 25 $cm^3$, catalyst loading: 1 g, catalyst particle size: 35–80 meshes. Used decalin had 37.5% cis isomer and a trans/cis ratio 1.63. It was found that after a few minutes the attrition action of the stirrer reduced the catalyst to a powdery slurry that after drying would mostly pass through a 200 meshes sieve. With this particle size and the high stirring rate it was assumed that diffusional limitations to mass transfer were eliminated. This was further confirmed by calculating the Weisz-Prater modulus ($\Phi = 0.06 \ll 1$). A sample was taken at the end of the experiments and it was analyzed using a Varian 3400 CX gas chromatograph equipped with a capillary column (Phenomenex ZB-5) and the FID. Previous identification of product studies were performed by GC–MS in a Saturno 2000 mass spectrometer coupled to a GC Varian 3800 using the same GC column.

## 3. Results and discussion

TPR profiles are shown in Fig. 1. The monometallic Ir(1.0) catalyst has a reduction peak centered at 183 °C and a shoulder at 200 °C which could be due to Ir oxide reduction. For higher Ir loadings (1.5) this peak is shifted to higher temperatures (198 °C) and is also widened due to a higher heterogeneity of surface Ir oxides or a more intense metal–support interaction. For monometallic Pt catalysts, the reduction peak is only slightly shifted to higher temperatures as the Pt loading increases (peaks centered at 167 °C and 171 °C for Pt(1.0) and Pt(1.5), respectively). A shoulder can also be observed in the reduction traces of these catalysts which extend up to 360 °C and is less pronounced for the Pt(1.5) catalyst. For the impregnated Pt/NaY sample. The second peak, a weaker band at 216 °C, could also arise from less accessible platinum. These results show some heterogeneity of the $Pt^{n+}$ ions in the Pt/NaY sample [21]. The TPR results demonstrate that monometallic Pt(1.5) has bigger crystals compared to Pt(1.0).

All bimetallic catalysts belonging to the Ir(1.0)Pt($y$) series displayed TPR profiles with two reduction peaks, one centered at 150–170 °C, and the other at 190–240 °C. These peaks were assigned to the reduction of Pt–Ir ensembles of different compositions [22,23]. The two peaks were also brought closer as the total

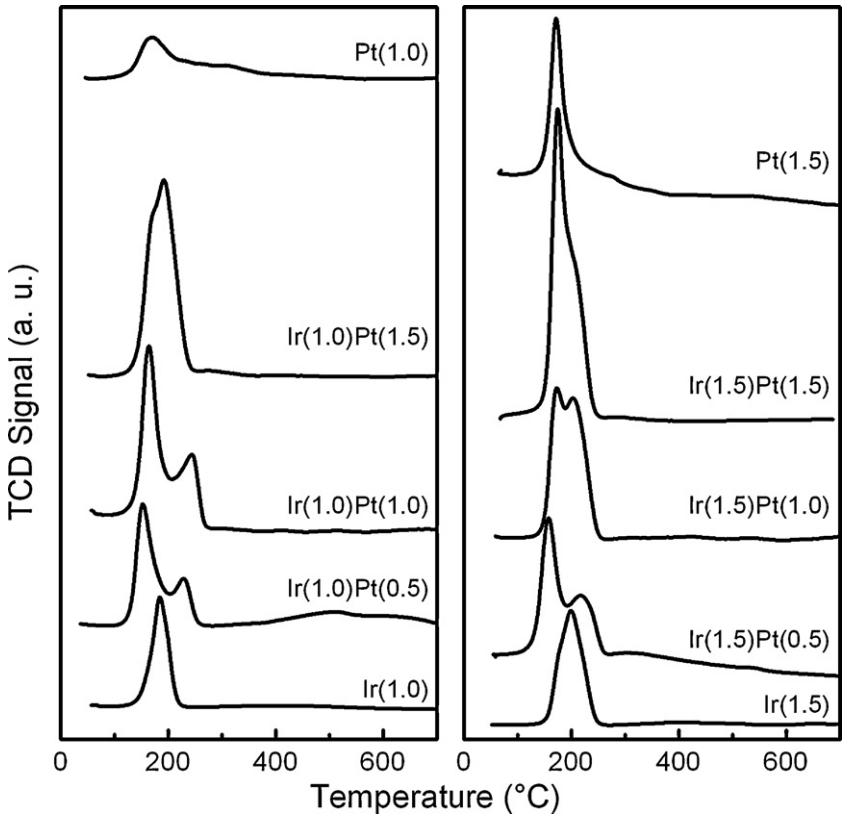


**Fig. 1.** Profiles of TPR Pt(1)Ir(0.5) and Pt(1.5)Ir(0.5) catalysts and of the series Ir(1)Pt($y$ = 0.5, 1, 1.5) and Ir(1.5)Pt($y$ = 0.5, 1, 1.5).

metal loading increased up to their virtual fusion. This behavior could be explained taking into account that for high metal loadings the metal precursors are adsorbed on weaker surface sites. The formation of Pt–Ir ensembles of lower dispersion was favored and in these ensembles Pt and Ir were simultaneously reduced. The behavior of Ir(1.5)Pt($y$) series was virtually the same.

Table 1 reports the maximum reduction temperatures. It is important to note that the hydrogen consumption (not shown) demonstrated the complete reduction of the metals contained in the zeolitic matrix. From the profiles in Fig. 1, it could be observed that the higher the metal content the more overlapping of the individual reduction peaks occurred, which suggests a higher interaction of metals.

In order to analyze the effect of the supported metals on the zeolitic acid sites, we obtained the FTIR spectra of the samples. Fig. 2 shows the OH region of the FTIR spectra. The spectra of the zeolitic matrix show two bands at 3557 and 3637 $cm^{-1}$ corresponding to OH species (Brønsted) associated to different positions into the zeolite [21,24,25]. The bands at 3672 and 3735 $cm^{-1}$ are attributed to extra-framework entities (EFAls and silanols). After the addition of metals (Ir and/or Pt) the spectra change drastically. Fig. 2A shows that a clear redistribution of Brønsted sites takes place in the monometallic samples and that the OH–FTIR bands are concentrated at 3603 $cm^{-1}$ together with a drop of intensity while the EFAl and silanols bands remain unchanged. The simultaneous presence of both metals in the zeolite leads to a very different spectrum, where there is no defined band associated with OH groups but there appears a width profile which suggests the presence of OH species dispersed in the matrix, modified by the presence of the metallic particles, probably interacting with each other.

The distribution of the acid sites into the zeolite is also affected by the Pt/Ir ratio. Fig. 2B shows the results obtained for the Ir(1.0)Pt(0.5) and Ir(1.0)Pt(1.0) catalysts. It can be seen that the lower the Pt/Ir ratio the lower intensity of the OH–FTIR region bands. We could suggest three hypotheses which may occur simultaneously or independently: (i) when the Pt content is low (Ir(1.0)Pt(0.5)) the particles strongly interact with the matrix, (ii) the Ir and Pt particles are highly dispersed, hindering the OH species; (iii) the impregnation of high amounts of Ir and Pt produced a partial collapse of the zeolite structure.

XRD spectra of the prepared catalysts were performed in order to check the occurrence of a possible zeolite structure collapse (iii). Fig. 3 shows the XRD spectra of the catalysts. It can be seen that only the Ir(1.5)Pt(1.5) suffered from a loss of the integrity of the zeolite structure. In all other cases the zeolite integrity was preserved, indicating that the acid concentration used for metal loading was correct: $H_2PtCl_6$ (0.077 N) and $H_2IrCl_6$ (0.04 N). In this sense Yan et al. [26] have reported that the HY zeolite structure is not changed by a treatment with nitric acid (0.25 N) using a proportion of 1 g zeolite per 20 ml solution at room temperature and under

**Table 1**
Maximum temperatures from $H_2$-TPR experiments, quantification of the areas from the pyridine desorption and the sodium content of the catalysts determined by atomic absorption spectroscopy.

| Catalysts | Maximum temperature (°C) | | Py-TPD[a] | Sodium (wt%) |
|---|---|---|---|---|
| NaY zeolite | | | | 7.52 |
| HY zeolite | | | 0.88 | 2.41 |
| Ir(1.0) | 183 | 200 (sh) | 1.30 | 2.40 |
| Ir(1.0)Pt(0.5) | 149 | 228 | 1.70 | 2.43 |
| Ir(1.0)Pt(1.0) | 166 | 243 | 2.17 | 2.38 |
| Ir(1.0)Pt(1.5) | 172 (sh) | 191 | 2.80 | 2.45 |
| Pt(1.0) | 166 | | 1.00 | 2.42 |
| Ir(1.5) | 174 (sh) | 208 | 1.62 | 2.39 |
| Ir(1.5)Pt(0.5) | 158 | 216 | 1.63 | 2.46 |
| Ir(1.5)Pt(1.0) | 169 | 203 | 2.90 | 2.36 |
| Ir(1.5)Pt(1.5) | 175 | 201 | 3.29 | 2.40 |
| Pt(1.5) | 168 | | 1.90 | 2.41 |

[a] Adsorption area referred to Pt(1.0).

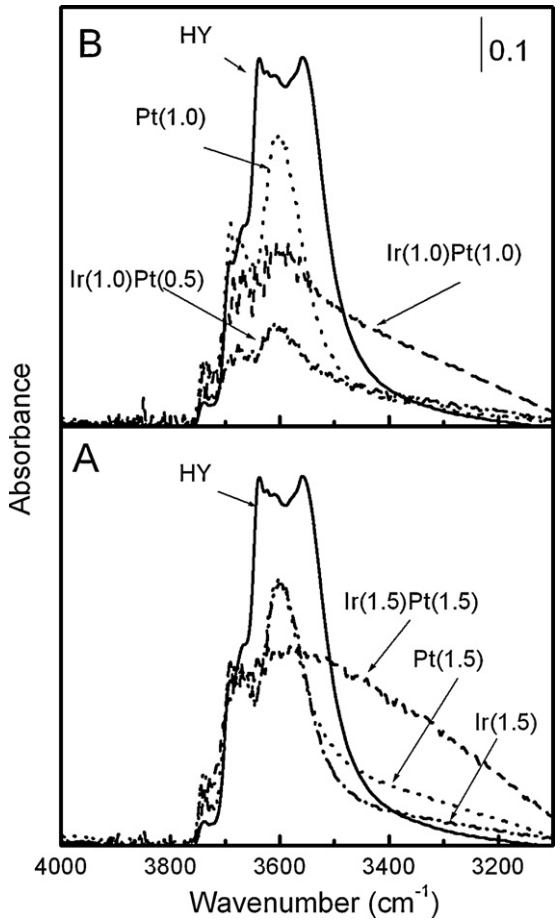


**Fig. 2.** FTIR OH-stretching bands of catalysts under study. (A) Catalysts containing 1.5 wt% of Ir: Ir(1.5), Pt(1.5) and Ir(1.5)Pt(1.5), comparison with HY. (B) Catalysts containing 1 wt% of Ir: Ir(1.0)Pt(1.0), Ir(1.0)Pt(0.5) comparison with HY and Pt(1.0).

reflux conditions for 8 h. The authors also report that nitric acid concentration values higher than 0.25 N produce a change of the XRD patterns. Under more severe leaching conditions ($\gg$0.25 N) the diffraction peaks become weaker and weaker, indicating a collapse of the framework structure, while the broad peak due to the amorphous phase (silica–alumina) becomes more and more important. Yan et al. [26] also observed a drastic change of the catalyst activity that correlated with the collapse of the zeolite structure (cracking of n-dodecane decreased from 62% to 6.1%). The Ir(1.5)Pt(1.5) catalyst however had a similar catalytic performance for SRO of decalin though an anomalous behavior for CH dehydrogenation and CP hydrogenolysis.

To further investigate the effect of Pt and Ir supported on the HY zeolite and find whether there is any real interaction between Pt and Ir, we analyzed the FTIR spectra of CO adsorbed on the catalysts prepared.

It is widely known that CO adsorption on metal modified zeolites presents several FTIR bands due to the contribution of the species associated with the zeolitic structure and with each metal [27]. The adsorption of CO on $Ir/Al_2O_3$ was studied by Solymosi et al. [28]. They attributed the Ir°–CO complexes to a band at 2080–2050 $cm^{-1}$. On the other hand, the CO adsorbed on Pt° supported in several matrixes gave rise to a band at 2060 $cm^{-1}$, that could be shifted up to 2100 $cm^{-1}$, typical of the linear carbonyls of Pt°, while bridging carbonyls can be observed at about 1850 $cm^{-1}$ [27].

Some authors reported results of CO adsorption on zeolites modified with platinum. Jaeger and Schulz-Eldoff [29] speculated about the existence of two types of Pt particles in Pt/KL zeolite catalysts. The first one is localized on the outer surface of the zeolite microcrystals or at near surface locations; CO adsorbed on these particles has absorption bands at 2060–2050 $cm^{-1}$, close to those found in Pt dispersed on conventional supports. The particles of the second group are supposed to be encaged inside zeolite channels so their electronic structure is presumably strongly perturbed by the surrounding zeolite framework. CO adsorbed on these Pt particles exhibits coverage dependent bands at frequencies in the 1960–1920 $cm^{-1}$ range. The marked downward shift

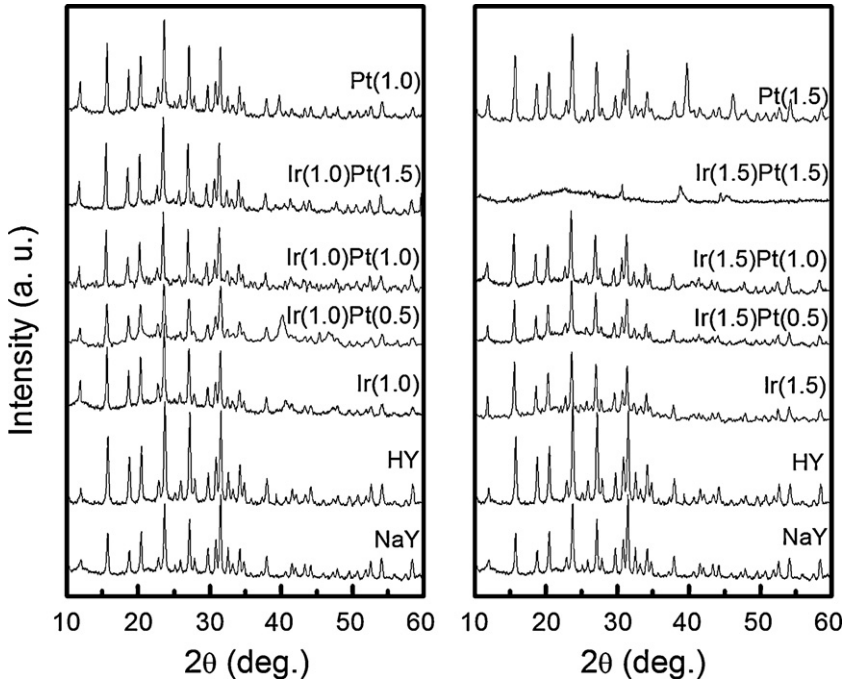


**Fig. 3.** XRD spectra of the catalysts and of the support.

**Table 2**
Main FTIR bands of adsorbed CO and suggested assignments.

| Band position ($cm^{-1}$) | Assignment | Catalysts ordered according to decreasing intensity of band |
|---|---|---|
| 3735 | Non-framework Si–OH hydroxyl groups | Pt(1.5) ≅ Ir(1.5)Pt(1.5) > Pt(1.0) ≅ Ir(1.5) > Ir(1.0)Pt(0.5) > HY |
| 3672 | Non-framework Al–OH hydroxyl groups | HY > Pt(1.0) > Pt(1.5) ≅ Ir(1.5) |
| 3637 | Species Brønsted associated to different positions into the zeolite | HY |
| 3557 | | |
| 3603 | Stretching vibration of acidic hydroxyl groups: Brønsted acids or bridging Si(OH)Al | Pt(1.0) > Pt(1.5) ≅ Ir(1.5) > Ir(1.0)Pt(0.5) |
| 2086 | $Ir^0$–CO (linear) the larger particle size, the higher the frequency | Ir(1.5) |
| 2070 | | |
| 2086 | $Pt^0$–CO (linear) the larger particle size, the higher the frequency | Pt(1.5) |
| 1637 | CO–OH (OH groups from matrix) | Ir(1.5) ≅ HY ≫ Ir(1.5)Pt(1.5) > Pt(1.0) > Ir(1.0)Pt(0.5) > Pt(1.5) > Ir(1.0)Pt(1.0) |

of these CO bands is attributed to the increase of electron density of these particles. Some authors [30–32] suggest that bands at about 2000 $cm^{-1}$ correspond to the well-dispersed small metal particles with more support interaction. At high loadings, the shift of the peaks clearly indicates the alloying effect. Platinum is in $Pt^0$ states [33,34] after the reduction which was confirmed by the peak observed at 2070 $cm^{-1}$. A detailed description of the adsorbed CO FTIR bands and their assignments is included in Table 2.

Fig. 4A reports the main bands that appear after the contact of 30 Torr of CO with the solids containing 1.5 wt% of Pt and/or Ir. On the Ir(1.5) catalyst the band at 2070 $cm^{-1}$ is assigned to CO linearly adsorbed on $Ir^\circ$. The presence of two shoulders at 2086 and 2032 $cm^{-1}$ may be due to $Ir^\circ$ at different locations into the matrix

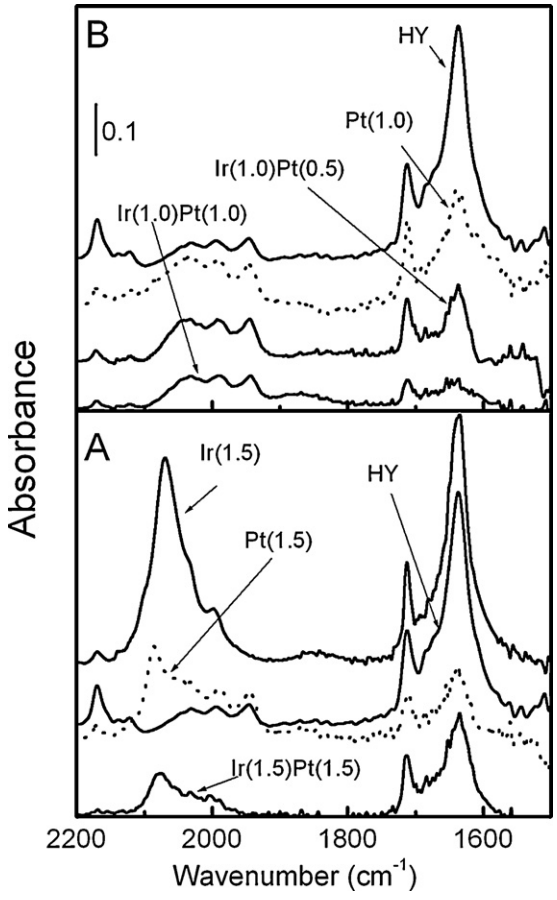


**Fig. 4.** Study by FTIR of the effect of the metal content on the CO (30 Torr) adsorption of the prepared catalyst and the support. (A) Catalysts containing 1.5 wt% of Ir: Ir(1.5), Pt(1.5) and Ir(1.5)Pt(1.5), comparison with HY. (B) Catalysts containing 1 wt% of Ir: Ir(1.0)Pt(1.0), Ir(1.0)Pt(0.5) comparison with HY and Pt(1.0).

or to the presence of inhomogeneous particle size distribution. The spectra obtained with the Pt(1.5) solid denote the presence of $Pt^\circ$ with the band at 2086 $cm^{-1}$. Finally, in the bimetallic catalysts, the adsorption band at 2077 $cm^{-1}$ can be associated with metallic particles. It should be noted that this band shifted to an intermediate value between the bare Pt and Ir. This observation together with the lower intensity may confirm our expectation about Pt–Ir interaction.

The band at 1637 $cm^{-1}$ can be associated with the adsorption of CO on the support surface ($\nu_{CO-OH}$), as this band also appears on the reduced HY without any supported metallic particle.

The intensity of the band at 1637 $cm^{-1}$ changes with the presence of the metal particles. For the Ir(1.5) solid, the intensity remains unchanged compared with the support, while when platinum is present (Pt(1.5) and Ir(1.5)Pt(1.5)) the signal drastically decreases. This behavior may be explained by the different particle sizes present in each catalyst together with the metal interaction in the bimetallic solid. Probably, at higher particle size, CO has lower accessibility to be adsorbed on the OH sites or, on the contrary, highly dispersed small metallic particles may cover the OH terminal species.

Fig. 4B shows the spectra obtained for the catalysts containing 0.5 and 1.0 wt% of platinum and 1.0 wt% of iridium. It is noticeable that in the 2200–1800 $cm^{-1}$ spectrum zone, the bands corresponding to CO adsorption on metal particles is negligible, while it remains the typical signal of the support. On the other hand, the band at 1637 $cm^{-1}$ due to $\nu_{CO-OH}$ shows a clear dependence with the metal content, showing the lower intensity for the Ir(1.0)Pt(1.0) and the higher for the Pt(1.0) solid. Again, we can conclude that there is a metal–metal interaction leading to the loss of the CO adsorption capacity on metallic sites or, probably, the size of the formed particles makes CO inaccessible to the adsorption sites.

These results seem to disagree with the spectra obtained in the 3200–4000 $cm^{-1}$ range, where the intensity of the isolated Brønsted sites decreases only when both metals are present. But it is important to take into account that the CO interaction with the adsorption species drastically depends on the surroundings of the OH groups and the consequent interactions.

On the other hand, the absence of the signal in the 2020–1800 $cm^{-1}$ range indicates the lack of bridged CO bonding with platinum or iridium, forming a $Pt^\circ$–CO–$Pt^\circ$ or $Ir^\circ$–CO–$Ir^\circ$ complex with different co-ordinations. This behavior reveals the low dispersion of metal particles in all the catalysts under study.

When a base like pyridine is adsorbed on an acid surface, strong bonds occur between the molecules adsorbed and the acid sites and high temperatures are needed in order to desorb the base. The measurement of the amount of base evacuated as a function of programmed heating temperature gives a measure of the acid strength distribution. Pyridine TPD patterns corresponding to Brønsted and Lewis acid sites are shown in Fig. 5 and the normalized areas are reported in Table 1. The sodium content of zeolites and catalysts

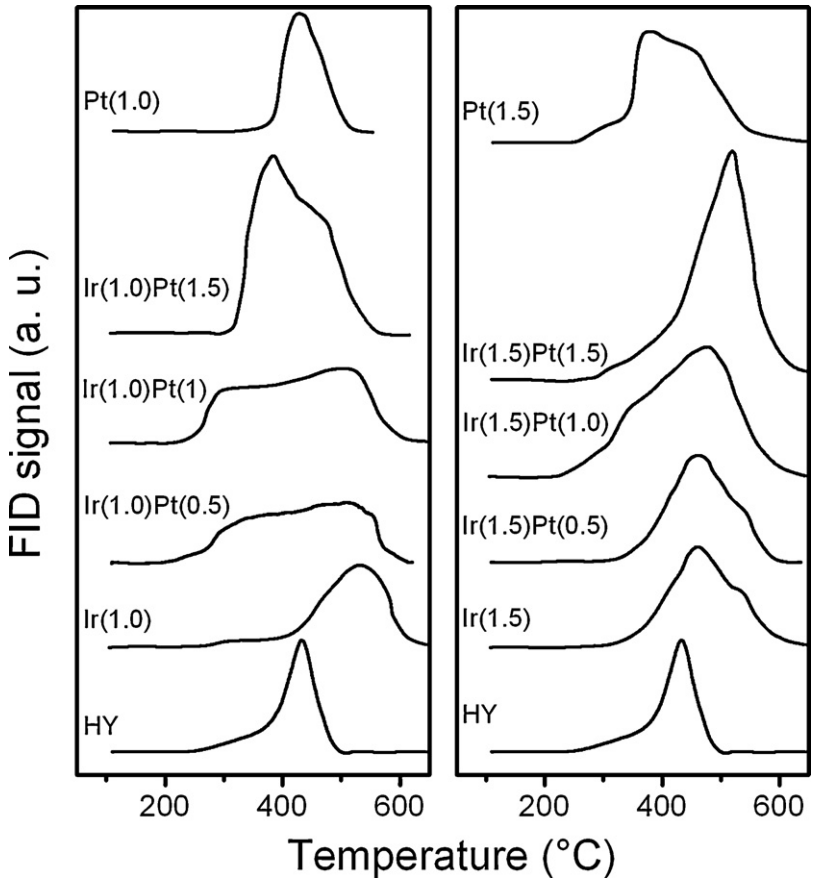


**Fig. 5.** Profiles of TPD of pyridine Pt(1)Ir(0.5) and Pt(1.5)Ir(0.5) catalysts and of the series Ir(1)Pt($y$ = 0.5, 1, 1.5), Ir(1.5)Pt($y$ = 0.5, 1, 1.5) and HY zeolite.

were also included due to its known influence on the acidity. It can be seen that after exchanging the support with aqueous $NH_4Cl$ the sodium content decreases from 7.52 wt% to 2.41 wt% and that the subsequent impregnation with Ir and/or Pt acid solutions does not produce any significant changes on the Na concentration level. Ammonium exchange of alkaline zeolites is a well known procedure to obtain its protonic forms. As the sodium contents are almost the same for all the catalysts the differences in the acidity are not due to sodium content.

It can be seen from Fig. 5 that the exchanged zeolite has only one desorption peak at 432 °C, a similar position as that reported by Dalla Costa and Querini [35]. When Ir is added to the HY matrix (1.0 or 1.5 wt%), the pyridine desorption peaks shift to higher temperatures, thus suggesting an increment in the acid strength. However, the presence of 1.0 or 1.5 wt% of platinum into the zeolitic matrix leads to a slightly shift to lower temperatures compared with HY. For the monometallic catalysts, the increase of metal loading produces an increase of the catalysts acidity. In the bimetallic catalysts, an increase in the area under TPD traces is observed as the Pt content increases for both Ir(1.0)Pt($y$) and Ir(1.5)Pt($y$) catalyst series. It is clear that at higher metal contents, the distribution of acid sites becomes more heterogeneous. Therefore, the acid strength of Ir catalysts appears to be higher than the one corresponding to Pt catalysts which is in agreement with the higher acidic character of Ir oxides. Changes in acid strength observed with the increase of the metal loading indicate that there is a preferential distribution of metals in the zeolite probably accompanied by some interaction between the metals and between the metals and the zeolitic matrix.

Nevertheless, the effect of a higher level of Ir loading is more important than that corresponding to increasing Pt loadings. It must be recalled again that as the total metal loading increases, the amount of high strength acidity decreases and, correspondingly, the amount of sites with intermediate acidity increases.

It can be seen from the FTIR–CO results that the presence of metal promoters decreases the Brønsted acidity. On the other hand, the measures of pyridine desorption show an increase of the total acidity. As a consequence, Pt and Ir increase the Lewis acidity.

Cyclopentane hydrogenolysis is a structure sensitive (demanding) reaction, so highly dispersed metals frequently have low activity [36]. The values of final conversions presented in Table 3 are in agreement with the higher hydrogenolysis of Ir as compared with Pt. The higher hydrogenolytic activity of Ir(1.5) series catalysts is noticeable as compared with that found for Ir(1.0) series catalysts despite the lower reaction temperature level used for the former series runs. Values of a deactivation parameter, defined as $(Xi - Xf)/Xi$, Xi and Xf being the initial and final conversions, respectively, are also shown in Table 3. It can be observed that the monometallic Pt catalysts suffer a more intense deactivation than the monometallic Ir ones. Deactivation is higher as the Pt loading increases for both bimetallic catalysts series, the deactivation being very low for the higher Ir loading series.

The values of mean conversion for cyclohexane (CH) dehydrogenation tests are also presented in Table 3. This reaction is structure insensitive and catalyzed by the metallic function [37]. As it can be observed, monometallic Pt catalysts have higher dehydrogenating activity than the Ir–HY catalysts. For both bimetallic catalysts series, cyclohexane conversion increases as the Pt loading increases. The bimetallic catalysts series with a lower Ir content has lower dehydrogenating activity than the solids with higher iridium content. It is somewhat unexpected that activity levels for the bimetallic catalysts with the highest Pt loading (1.5%) have only a third of activity as compared with the monometallic Pt one. This

**Table 3**
Values of final conversion, Xf, of cyclopentane (CP); parameter of deactivation of the catalyst in CP hydrogenolysis, (Xi – Xf)/Xi and conversion average of cyclohexane (CH).

| Catalyst | Cyclopentane hydrogenolysis | | Cyclohexane dehydrogenation, Xa (%) |
|---|---|---|---|
| | Xf (%) | (Xi – Xf)/Xi | |
| Ir(1.0) | 34.75 | 0.65 | 22.05 |
| Ir(1.0)Pt(0.5) | 82.00 | 0.18 | 28.46 |
| Ir(1.0)Pt(1.0) | 60.12 | 0.40 | 36.74 |
| Ir(1.0)Pt(1.5) | 49.60 | 0.90 | 37.29 |
| Pt(1.0) | 11.92 | 0.82 | 98.00 |
| Ir(1.5) | 98.05 | 0.02 | 23.28 |
| Ir(1.5)Pt(0.5) | 98.83 | 0.01 | 25.54 |
| Ir(1.5)Pt(1.0) | 97.41 | 0.02 | 27.29 |
| Ir(1.5)Pt(1.5) | 85.00 | 0.15 | 31.10 |
| Pt(1.5) | 5.34 | 0.85 | 98.60 |

Ir(1.0)Pt(*x*), Ir(1.0) and Pt(1.0) catalysts: mass = 150 mg, $T_{reaction}$ = 350 °C; Ir(1.5)Pt(*x*), Ir(1.5) and Pt(1.5) catalysts: mass = 100 mg, $T_{reaction}$ = 300 °C; Xf: conversion at 120 min time on stream; Xi: conversion at 5 min time-on-stream; Xa: average conversion.

proves that there exists a strong Pt–Ir metallic interaction, as indicated by TPR, pyridine adsorption and CP hydrogenolysis tests.

The results of the catalysts testing for decalin reaction are presented in Figs. 6 and 7. Values of decalin conversion and the percentage of cracking, ring contraction and ring opening products, naphthalene and other products at 300 °C and 350 °C are shown. The decalin reaction products were classified considering the criterion used by Santikunaporn et al. [38] and Chandra Mouli et al. [39]. The products of reaction are lumped according to:

*Cracking products ($C_1$–$C_9$ products):* 2-methyl butane, hexane, 2,3-dimethyl pentane, 3-methylpentane, 5-methyl, 1-hexene, methylcyclopentane, propylcyclopentane, 2-methylpropylcyclopentane, 1,1-dimethylcyclopentane, cyclohexane, methylcyclohexane, propylcyclohexane, cis 1-ethyl-2-methylcyclohexane, trans 1-ethyl-4-metilcyclohexane, 1-ethyl-3-methylcyclohexane, 1,1,4-trimethylcyclohexane;
*Ring opening (RO) $C_{10}$ products*: alkylcyclohexanes, alkylcyclopentanes cyclohexenes or benzenes (for example: 1-methyl-2-propylcyclohexane, diethylcyclohexane, cis and trans 1,1,3,5-tetramethylcyclohexane, 2-methylpropylbenzene);
*Ring contraction (RC) products:* 2,2,3-trimethyl bicyclo[2.2.1] heptane, 2,6,6-trimethyl bicyclo[3.1.1]heptane, 1,1′bicyclopentyl, spiro[4.5]decane, 3,7,7-trimethyl bicyclo[4.1.0]heptane;
*Other products:* 1-methylindan, cis and trans decahydronaphthalene, 1,2-dihydronaphthalene, 1,2,3,4-tetrahydronaphthalene and includes others heavy dehydrogenation products.

Main products of the RO reaction included in Fig. 6 are alkylcyclohexanes and alkylcyclopentanes, which are formed first. The "other products" group includes heavy dehydrogenation products.

The results shown in Fig. 6 reveal that at 300 °C all bimetallic catalysts of the Ir(1.0) series have lower percentages of RO products than the monometallic Pt one. The activity of monometallic Ir(1.0) catalysts is lower as compared with the monometallic Pt(1.0) catalyst, but this order is reversed for the ones with higher metal content (1.5). This phenomenon can be explained by considering that Pt(1.5) has a bigger crystal than the Pt(1.0) catalyst (i.e. lower amount of Pt superficial) as found by TPR. From these results,

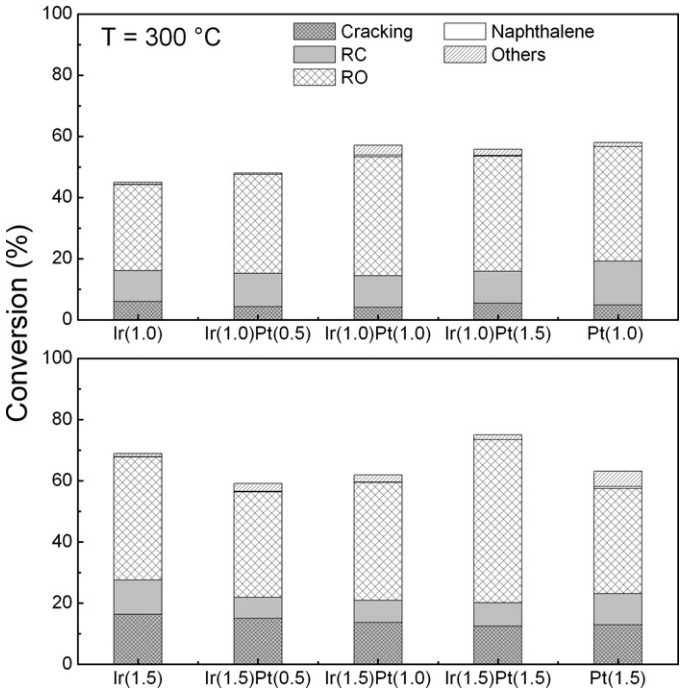


**Fig. 6.** Percentage of conversion of decalin to 6 h of reaction divided in cracking products, ring contraction (RC), ring opening (RO), naphthalene and others (heavy dehydrogenation products); $T_{reaction}$ = 300 °C.

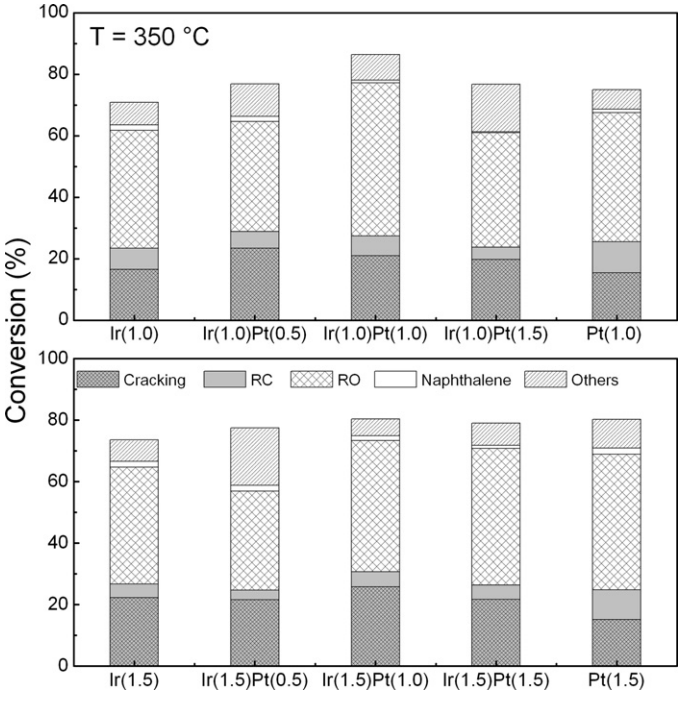


**Fig. 7.** Percentage of conversion of decalin to 6 h of reaction divided in cracking products, ring contraction (RC), ring opening (RO), naphthalene and others (heavy dehydrogenation products); $T_{reaction}$ = 350 °C.

**Table 4**
Conversion of decalin at 6 h of reaction, cis decalin and relation trans/cis decalin; selectivity to ring opening products. $T_{reaction}$ = 300 and 350 °C. Relation trans/cis decalin of reagent = 1.63; cis-decalin, % = 37.5.

| Catalyst | Cis decalin (%) | | Trans/cis decalin ratio | | Selectivity to RO | |
|---|---|---|---|---|---|---|
| | 300 °C | 350 °C | 300 °C | 350 °C | 300 °C | 350 °C |
| Ir(1.0) | 4.25 | 2.16 | 11.95 | 12.53 | 62.50 | 54.12 |
| Ir(1.0)Pt(0.5) | 4.52 | 2.48 | 10.51 | 11.03 | 67.35 | 46.54 |
| Ir(1.0)Pt(1.0) | 3.58 | 0.86 | 11.02 | 12.14 | 68.22 | 57.55 |
| Ir(1.0)Pt(1.5) | 3.92 | 1.86 | 10.03 | 11.49 | 67.53 | 48.52 |
| Pt(1.0) | 3.82 | 2.68 | 7.91 | 8.34 | 64.55 | 55.94 |
| Ir(1.5) | 2.13 | 1.86 | 13.57 | 13.23 | 58.42 | 51.74 |
| Ir(1.5)Pt(0.5) | 3.38 | 2.66 | 11.08 | 11.49 | 58.43 | 41.63 |
| Ir(1.5)Pt(1.0) | 3.46 | 1.41 | 10.01 | 12.94 | 62.36 | 53.07 |
| Ir(1.5)Pt(1.5) | 2.19 | 1.64 | 10.42 | 11.79 | 71.07 | 56.20 |
| Pt(1.5) | 3.12 | 1.24 | 10.80 | 14.9 | 54.43 | 54.85 |

it could be claimed that Ir(1.5)Pt($y$) catalysts have a better performance than Ir(1.0)Pt($y$) ones at 300 °C. Only the Ir(1.5)Pt(1.5) catalyst has a better performance than the monometallic catalysts in this series at 300 °C. In all cases, the formation of heavy dehydrogenation products is low, being higher for the monometallic Pt(1.5) catalyst.

The results included in Fig. 7 show that monometallic catalysts with higher metal loadings have higher activity for ring opening. On the other hand, the formation of naphthalene and heavy dehydrogenation products is much more important at this temperature level for both catalyst series. Reaction temperatures higher than 350 °C are thermodynamically unfavorable for SRO reactions because metal-catalyzed dehydrogenation dominates [40]. Cracking products become more important at 350 °C, and for both temperature levels bimetallic catalysts of higher Ir loadings produce more cracking products. The bimetallic Ir(1.0)Pt(1.0) catalyst has an outstanding performance at his temperature, with high decalin conversion and good yield to RO products.

Table 4 shows the cis-decalin percentage, the trans/cis decalin ratio and the selectivity to RO products at 6 h of time-on-stream for both temperature levels. Cis-decalin is more selectively converted to RO products than trans-decalin, which is converted mainly to cracking products [38]. Cis-decalin percentages are lower for bimetallic Ir(1.5)Pt($x$) catalysts as compared with Ir(1.0)Pt($x$) series ones at 300 °C. It should then be expected that as more cis-decalin disappear, more RO products should be formed. On the contrary, the experimental results indicate a higher selectivity toward RO products for Ir(1.0)Pt($y$) catalysts. At 350 °C cis-decalin percentages are lower mainly due to the higher conversion levels. The same trend for all bimetallic catalysts (i.e. lower cis-decalin levels for higher Ir level catalysts) was observed, with the exception of the Ir(1.0)Pt(1.0) catalyst which had the lowest cis-decalin percentage. It must be recalled here that decalin used as reactant had a 1.63 trans/cis ratio value, and this ratio increased as the reaction proceeded. Higher trans/cis decalin ratios could be due to a higher reactivity of the cis isomer and also to the catalytic cis/trans isomerization reaction [41].

Reaction products obtained with Pt monometallic catalysts have a lower cis/trans decalin ratio than the corresponding Ir ones. This ratio has intermediate values in reaction products obtained with bimetallic Pt–Ir catalysts. The observed increase in trans/cis ratio at the highest temperature level could be due to a higher reactivity of the cis isomer. Chandra Mouli et al. [40] found that stereoisomerization is an important step in decalin RO reaction. RO products selectivity is higher at 300 °C than at 350 °C for both bimetallic catalysts series. Notwithstanding, the yield of RO products is better at the highest temperature level due to the increased activity of catalysts.

RO products are mostly produced in the catalysts with the same Pt/Ir atomic ratio at both reaction temperatures (300 and 350 °C). Chandra Mouli et al. [40] found that the optimum Pt/Ir ratio was 0.5 for getting a maximum ring opening yield of 16 wt% and a selectivity of 26 wt% from decalin at 350 °C. The difference can be attributed to a different support used by Chandra Mouli et al. [40], namely Zr modified MCM-41.

## 4. Conclusions

The deposition of Pt and Ir on the HY zeolite increases the amount of total acid sites and modifies the acid strength distribution of this support. The addition of Ir increases the amount of high strength sites and that of Pt has the same effect on moderate strength acidity while the total acidity is increased. On the other hand, the Brønsted acidity is decreases.

Bimetallic catalysts with higher Ir content have more hydrogenolytic activity, which is in agreement with the higher hydrogenolytic activity of Ir as compared with Pt. An increase of the Pt content decreases the activity for both bimetallic catalysts series, and the catalysts of the Ir(1.5)Pt($y$) series virtually do not suffer a significant deactivation (possibly due to an enhanced hydrogenolysis of coke precursors) upon CP hydrogenolysis.

XRD results indicate that the zeolite structure is only affected by impregnation with acid solutions at high concentrations of Ir and Pt (only Ir(1.5)Pt(1.5) catalyst was affected). In any case changes in the zeolite structure do not affect the catalytic activity significantly.

An increase in the Pt content of catalysts favored their hydrogenating activity but no similar correlation was found for the formation of dehydrogenated products in decalin transformation.

The TPR results indicate that the Pt–Ir metallic interaction seems to be more intense for catalysts with an atomic Pt/Ir ratio of 1. Such catalysts exhibit an adequate metal/acid balance and are suitable for naphthenic ring opening, mainly the low total metal content one.

## References

[1] B.H. Cooper, B.B.L. Donnis, Appl. Catal. A 137 (1996) 203–223.
[2] N.T. Tam, R.P. Cooney, G. Curtheoys, J. Catal. 44 (1976) 81–86.
[3] G. Onyestyák, G. Pál-Borbély, H.K. Beyer, Appl. Catal. A 229 (2002) 65–74.
[4] G.B. McVicker, M. Daage, M.S. Touvelle, C.W. Hudson, D.P. Klein, W.C. Baird Jr., B.R. Cook, J.G. Chen, S. Hantzer, D.E.W. Vaughan, E.S. Ellis, O.C. Feeley, J. Catal. 210 (2002) 137–148.
[5] A. Corma, F. Mocholi, A.V. Orchillés, G.S. Koermer, R.J. Madon, Appl. Catal. 67 (1991) 307–324.
[6] H.S. Cerqueira, P.C. Mihindou-Koumba, P. Magnoux, M. Guisnet, Ind. Eng. Chem. Res. 40 (2001) 1032–1041.
[7] J. Abbot, J. Catal. 123 (1990) 383–395.
[8] J.A. Martens, P.A. Jacobs, Stud. Surf. Sci. Catal. 137 (2001) 633–671.
[9] F.C. Jentoft, B.C. Gates, Top. Catal. 4 (1997) 1–13.
[10] Y. Ono, Catal. Today 81 (2003) 3–16.
[11] A. Corma, P.J. Miguel, A.V. Orchillés, J. Catal. 145 (1994) 171–180.
[12] S.T. Sie, Ind. Eng. Chem. Res. 32 (1993) 397–402.
[13] M.V. Frash, R.A. van Santen, Top. Catal. 9 (1999) 191–205.
[14] A.M. Rigby, G.J. Kramer, R.A. van Santen, J. Catal. 170 (1997) 1–10.

[15] M.A. Arribas, A. Martınez, Appl. Catal. A 230 (2002) 203–217.
[16] A. Corma, V. Gonzalez-Alfaro, A.V. Orchillés, J. Catal. 200 (2001) 34–44.
[17] T.V. Vasina, O.V. Masloboishchikova, E.G. Khelkovskaya-Sergeeva, L.M. Kustov, Stud. Surf. Sci. Catal. 138 (2001) 93–100.
[18] D. Kubicka, N. Kumar, P. Maki-Arvela, M. Tiitta, V. Niemi, H. Karhu, T. Salm, D.Y. Murzin, J. Catal. 222 (2004) 65–79.
[19] D. Kubicka, N. Kumar, P. Maki-Arvela, M. Tiitta, V. Niemi, H. Karhu, T. Salm, D.Y. Murzin, J. Catal. 227 (2004) 313–327.
[20] M.A. Arribas, P. Concepción, A. Martínez, Appl. Catal. A 267 (2004) 111–119.
[21] K. Chakarova, K. Hadjiivanov, G. Atanasova, K. Tenchev, J. Mol. Catal. A 264 (2007) 270–279.
[22] U. Nylén, J.F. Delgado, S. Järås, M. Boutonnet, Appl. Catal. A 262 (2004) 189–200.
[23] C.M.N. Yoshioka, T. Garetto, D. Cardoso, Catal. Today 107–108 (2005) 693–698.
[24] T. Montanari, O. Marie, M. Daturi, G. Busca, Catal. Today 110 (2005) 339–344.
[25] L. Gutierrez, E. Lombardo, Appl. Catal. A 360 (2009) 107–119.
[26] Z. Yan, D. Ma, J. Zhuang, X. Liu, X. Liu, X. Han, X. Bao, F. Chang, L. Xu, Z. Liu, J. Mol. Catal. A: Chem. 194 (2003) 153–167.
[27] K.I. Hadjiivanov, G.N. Vayssilov, Adv. Catal. 47 (2002) 307–511.
[28] F. Solymosi, E. Novak, A. Molnar, J. Phys. Chem. 94 (1990) 7250–7255.
[29] N.I. Jaeger, G. Schulz-Eldoff, Catal. Lett. 32 (1995) 147–158.
[30] F. Solymosi, J. Rasko, J. Catal. 62 (1980) 253–263.
[31] F. Solymosi, J. Rasko, J. Catal. 63 (1980) 217–225.
[32] A. Erdohelyi, K. Fodor, G. Suru, Appl. Catal. A 139 (1996) 131–147.
[33] C. Mihut, C. Descorme, D. Duprez, M.D. Amiridis, J. Catal. 212 (2002) 125–135.
[34] M.M. Otten, M.J. Clayton, H.H. Lamb, J. Catal. 149 (1994) 211–222.
[35] B.O. Dalla Costa, C.A. Querini, Chem. Eng. J. 162 (2010) 829–835.
[36] J.M. Parera, N.S. Fígoli, in: G.J. Antos, A.M. Aitani, J.M. Parera (Eds.), Catalytic Naphtha Reforming Science and Technology, Marcel Dekker, New York, 1995 (Chapter 3).
[37] M. Boudart, Adv. Catal. 20 (1969) 153–166.
[38] M. Santikunaporn, J.E. Herrera, S. Jongpatiwut, D.E. Resasco, W.E. Alvarez, E.L. Sughrue, J. Catal. 228 (2004) 100–113.
[39] K. Chandra Mouli, V. Sundaramurthy, A.K. Dalai, J. Mol. Catal. A: Chem. 304 (2009) 77–84.
[40] K. Chandra Mouli, V. Sundaramurthy, A.K. Dalai, Z. Ring, Appl. Catal. A 321 (2007) 17–26.
[41] R.C. Schucker, J. Chem. Eng. Data 26 (1981) 239–241.